Journal of Applied Polymer Science

# High Thermal Conductive M-Xylylenediamine Functionalized Multiwall Carbon Nanotubes/Epoxy Resin Composites

**Fan Xie, Shuhua Qi, Rui Yang, Dong Wu**
Department of Applied Chemistry, School of Science, Northwestern Polytechnical University, Xi'an 710072 China
Correspondence to: S. Qi (E-mail: qishuhua@nwpu.edu.cn)

**ABSTRACT:** In this study, multiwall carbon nanotubes (MWNTs) functionalized by m-xylylenediamine is used as thermal conductive fillers to improve their dispersibility in epoxy resin and the thermal conductivity of the MWNTs/bisphenol-A glycidol ether epoxy resin composites. Functionalization with amine groups of MWNTs is achieved after such steps as carboxylation, acylation and amidation. The thermal conductivity, impact strength, flexural strength, and fracture surfaces of MWNTs/epoxy composites are investigated with different MWNTs. The results show that m-xylylenediamine is successfully grafted onto the surface of the MWNTs and the mass fraction of the organic molecules grafted onto MWNTs is about 20 wt %. The thermal conductivity of MWNTs/epoxy composites is further enhanced to 1.236 W/mK with 2 wt % m-MWNTs. When the content of m-MWNTs is 1.5 wt %, the impact strength and flexural strength of the composites are 25.85 KJ/m$^2$, 128.1 MPa, respectively. Scanning electron microscope (SEM) results show that the fracture pattern of composites is changed from brittle fracture to ductile fracture. © 2014 Wiley Periodicals, Inc. J. Appl. Polym. Sci. **2015**, *132*, 41255.

**KEYWORDS:** composites; functionalization of polymers; graphene and fullerenes; nanotubes; properties and characterization

Received 12 March 2014; accepted 2 July 2014
**DOI: 10.1002/app.41255**

## INTRODUCTION

With further miniaturization and increasing power consumption of microelectronics devices, heat dissipation has become critical to their performance, reliability in the microelectronic systems. The high integration of transistors has resulted in the escalation of power dissipation as well as an increase in heat flux at the devices.[1,2] However, most common polymers for packaging such as epoxy, polyethylene, polyimide, and polyamide acrylonitrile-butadiene-styrene (ABS) etc., are often practically restricted by a low thermal conductivity. Among them, epoxy resin is widely used in electronic packaging materials, coatings, adhesives and one kind of thermosetting resin in the field of composite materials, which has excellent adhesion, chemical resistance and is an ideal matrix composite material. However, the poor thermal conductivity (0.2 W/mk) limits its applications such as printed circuit board, heat exchangers, thermal interface materials and phase change materials. Under this circumstance, highly thermal conductive polymers are emerging as one of the most economic and effective means to remove heat accumulated from microelectronics and to cope with thermal management issues.

Carbon nanotubes (CNTs)[3] have attracted much research interest due to their novel structures, excellent mechanical,[4,5] thermal,[6,7] and electrical properties.[8] The thermal conductivity of MWNTs can be twice as high as the diamond and the strength is two magnitude higher than the steel, which can be about 1 Tpa.[9] Owing to their unique properties, MWNTs are considered ideal candidates as reinforcing materials in polymer matrix. Introduction of MWNTs into polymers may improve their applications in the fields of reinforcing composites, electronic devices and so on.[10,11] In particular, these unique properties enable the development of thermal conductive polymers using very low filler contents without affecting the mechanical performance of the matrix, while the traditional filler like ceramic and metals need high concentration more than 50 vol %.[12]

Carbon nanotubes exhibit a high thermal conductivity (3000 W/mk) due to their consistence of carbon atoms assembled in a graphitic structure. Therefore, nanotube-reinforced epoxy systems hold the promise of delivering superior composite materials with high strength, light weight and multifunctional features.[13] However, there are two main problems needed to be solved during the realization of nanotube-reinforced resin. One major limit to the application of the MWNTs is the atomically smooth nonreactive surface of nanotubes, which can easily agglomeration due to Van der Waals force that will hold together in bundles resulting very poor dispersion in most solvents.[14,15] Another issue is that the lack of interfacial bonding limits load transfer from the matrix to

nanotubes. Therefore, the functionalization of MWNTs is necessary for further application.

Numerous methods including chemical reactions,[16,17] UV-ozone,[18] plasma,[19] microwave[20] functionalization at the tips or sidewall of carbon nanotubes have already been reported.[21,22] Most of the recent publications reported have a certain enhancement of the thermal conductivity of the polymer-based composites, by an incorporation of treated CNTs. Among them, amino-functionalized CNTs have been widely studied.[23,24] The application of conductive fillers to an isolating polymer matrix is expected to enhance the thermal properties to about 0.8 to 1.0 W/mk. Besides, a homogeneous dispersion and a strong adhesion to the matrix are also desired. However, the observed effects of the CNT-incorporation into the polymers and the influence of the functionalization on the thermal conductivity are not significant with low filler content. Generally results in poor heat dissipation only with $\lambda = 0.1–1.0$ W/mK with up to 50 wt % CNT loading.[25]

So in the present work, m-xylylenediamine (MPDA) was chosen as the functional molecule, which has a high reactivity, a wealth of chemistry, may act as a curing agent and react with the epoxy matrix to build a covalent linkage during the curing process.[26] The functionalization was performed via the reaction of terminal diamine with carboxyl groups attached to the MWNTs in the course of acylation treatment. The aim of the study is to investigate the influence of different MWNTs on thermal conductivity and the mechanical properties of the epoxy-based composites and the main factors affecting the thermal conductivity confirmed through theoretical analysis.

## EXPERIMENTAL

### Materials

As-received MWNTs (r-MWNTs; purity >95%) were supplied by Shenzhen Nanotech Port Co. Ltd., China. They were produced by the chemical vapor deposition method with 60 to 100 nm in diameter and 5to 15 $\mu$m in length. Epoxy resin utilized in this work was a nominally difunctional epoxy resin, bisphenol-A glycidol ether epoxy resin (DGEBA), supplied by Lan Xing New Material Wuxi Resin Co.; 2-ethyl-4-methylimidazole (EMI-2,4) acted as a curing agent and was provided by Sinopharm Chemical Reagent Co., Ltd. M-xylylenediamine was obtain from Huaian Institute of curing agent, Xing Huai, China. Acetone and *N*,*N*-dimethylformamide (DMF) were received from Tianjin Fu Yu Fine Chemical Co., Ltd. Ethanol and thionyl chloride ($SOCl_2$) were supplied by Tianjin Fucheng Chemical Reagent. $H_2SO_4$ (AR, 96–98%) was purchased from Daxing District Industrial. $HNO_3$ (AR, 65–68%) was supplied by West Long Chemical Co., Ltd. Shantou. Tetrahydrofuran (THF) was provided by Tianli Chemical Reagent Co., Ltd., Tianjin.

### Chemical Functionalization of MWNTs

**Carboxyl-Functionalization of MWNTs.** The functionalization process of MWNTs is shown in Figure 1. Before the MPDA molecule was grafted onto the surface of MWNTs, acid modification of MWNTs was the key step to effectively generate carboxyl groups on the surface. Compared with effectiveness of all the acid treatment methods, the one described as follows was chosen finally.

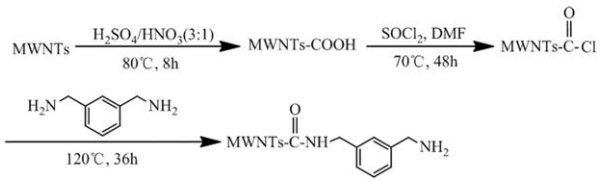


**Figure 1.** Scheme for the process of the amino functionalization of MWNTs.

First, high temperature treatment was employed. Certain amount of as-received MWNTs were put in a muffle furnace at 400°C for several hours followed by furnace cooling in order to remove impurities and the amorphous carbon sufficiently. Then obtained MWNTs were added into the three-necked flask, and then added a volume fraction of 3 : 1 mixture of concentrated $H_2SO_4/HNO_3$, refluxed at 80°C for some time. The carboxylated MWNTs were filtered with mixed cellulose membrane filtration and washed with deionized water until pH was 7 and dried in vacuum oven 80°C for 24 h. The resulting material is defined as a-MWNTs.

**Amino-Functionalization of MWNTs.** A-MWNTs were dissolved in DMF, adding an excess of thionyl chloride after ultrasonic dispersion, then kept 70°C for a certain period of time under mechanical stirring, washed with THF to remove excess thionyl chloride, dried 12 h at 60°C, finally chloride MWNTs were obtained. The resulting material is defined as c-MWNTs.

The c-MWNTs were dissolved in DMF until dispersed uniformly, adding an excess of m-xylylenediamine. The mixture was stirred 36 h at 120°C under the protection of nitrogen. After cooling to room temperature, the MWNTs were washed with ethanol and THF for five times to remove excess diamine. Finally, the black solid was dried at room temperature overnight under vacuum. The resulting material is defined as m-MWNTs.

### Preparation of MWNTs/Epoxy Composites

The r-MWNTs, a-MWNTs, m-MWNTs were dispersed in acetone (2 mg/mL) by an ultrasonicator bath for 30 min. The dispersion was mixed with DGEBA and the ratio of MWNTs/DGEBA mixture was adjusted for the different content of MWNTs. The mixture was placed in a warm sonicator bath at 65°C until most of the solvents were removed and then evacuated all solvents. Subsequently, appropriate amount of the curing agent was added and stirred to get good homogeneity and to accelerate the evaporation of acetone, and then placed in a vacuum oven at 60°C for continuous vacuum in order to completely remove the solvent and get rid of air bubbles. Finally, the mixture was poured into a mould and the whole system was placed in an oven. The MWNTs/DGEBA/EMI-2,4 was precured at 70°C for 3 h, cured at 110°C for 1 h, and postcured at 150°C for 3 h to form MWNTs/epoxy composites.

### Instrumental Analysis

Infrared Spectra were obtained using a WQF-310 type Fourier transform infrared (FT-IR) spectrometer manufactured by Beijing Second Optical Instrument Factory. The MWNTs samples

were ground into powder, and then KBr pellets were prepared with the MWNTs. The spectrum was collected in the range from 4000 to 400 $cm^{-1}$. The changes of the group in matrix can be obtained by using the Fourier transform infrared spectroscopy. The resolution of apparatus was 4 $cm^{-1}$, the number of scans was 16 times. The phase structures of the MWNTs were detected by X-ray powder diffraction (XRD; X' Pert Pro model, Holland) with the scanning rate of 5°/min. The X-ray patterns for $2\theta$ from 10° to 80° were obtained. The morphological observations were executed using a field emission scanning electron microscope (FESEM)(JSM-6360LV, Japan). The fracture toughness property of pure cured epoxy resin and MWNTs/epoxy composites was evaluated from the impact strength. The samples were sputtered with gold in vacuum prior to observation. The observation was carried out on the cross-sections of samples. Charpy impact tests were performed on an impact tester (BC-50) with impact energy of 5 J at room temperature in accordance with GB/T2571-1995. The specimen dimensions were 80 mm × 10 mm × 4 mm. Five specimens were tested for each set of conditions and the mean value was calculated. The flexural tests were carried out following GB/T2570-1995. Five specimens were tested and averaged for each sample. The dimensions of the specimens were the same as the impact specimens. The specimens were loaded in three-point bending until failure at room temperature on a universal testing machine (SANS-CMT5105). Transmission electron microscopy (TEM) was taken on H800-type (Hitachi Co.) to characterize the microstructures of MWNTs. The thermal property of the functionalized-MWNTs were analyzed using a thermo gravimetric analyzer (TGA, Q-50, TA, America,) with a heating rate of 10°C/min in the range from 25 to 700°C under nitrogen atmosphere. Thermal conductivity measurement was conducted by employing a Hot Disk thermal analyzer (Hot Disk AB, Uppsala/Sweden) using the transient place source (TPS) method. A disk-shaped TPS sensor with a diameter of 7 mm and a thickness of 0.07 mm was placed between two circular sample pieces with diameters of 20 mm and thicknesses of 2 mm. The upper surface and under surface were polished by fine sand paper prior to use.

## RESULTS AND DISCUSSION

### FT-IR Characterization

In our study, FT-IR was utilized to identify the specific functional groups on the MWNTs as an evidence of the grafting of MPDA. Figure 2 shows the FT-IR spectra of as received MWNTs, carboxyl-MWNTs, and the amino-MWNTs. IR spectrum peaks of the pristine MWNTs are more complex. This is because there exists some metal impurities and amorphous carbon in it. Figure 2(a) suggests that the absorption peaks around 3440 $cm^{-1}$ are associated with vibration of the –OH group, which is due to a certain amount of water in MWNTs. The absorption peaks around 2360 $cm^{-1}$ correspond to carbon dioxide. Compared with the pristine MWNTs, the carboxyl-MWNTs spectra shown in Figure 2(b) indicate that the absorption peak around 3440 $cm^{-1}$ is more stronger and the new adsorption at 1634 $cm^{-1}$ is the characteristic for asymmetric stretching vibration of the –COOH bond, where the signal at 1168 $cm^{-1}$ is assigned to the stretching vibration absorption of

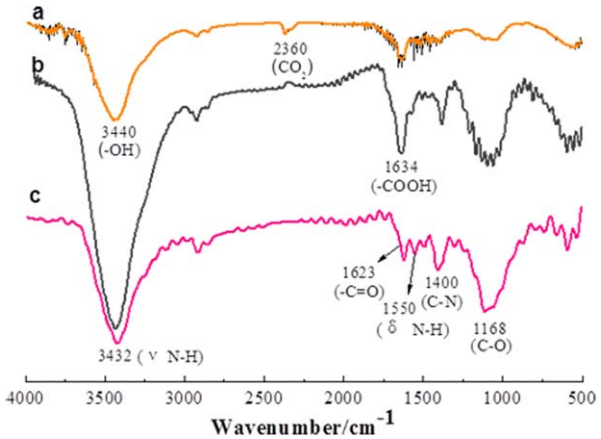


**Figure 2.** FT-IR spectra of different MWNTs (a), r-MWNTs (b), a-MWNTs (c), m-MWNTs. [Color figure can be viewed in the online issue, which is available at wileyonlinelibrary.com.]

C–O bond of the –COOH bond.[27] It is suggested that the hydroxyl and carboxyl groups are successfully introduced onto the sidewalls of the MWNTs under the strong acid oxidation. Figure 2(c) indicates that peaks around 1623 $cm^{-1}$ correspond to stretching vibration of the carboxyl band I absorption in the imide group. The absorption peak around at 3432 $cm^{-1}$ is associated with the stretching vibration absorption of the N–H bond[28,29] and the peak around 1550 $cm^{-1}$ correspond to the bending vibration absorption of the N–H bond in the secondary amide.[30] The signal at 1400 $cm^{-1}$ is assigned to the stretching vibration absorption of the C–N bond. From the FT-IR spectrum of Figure 2, we can speculate that the active chemical groups of MPDA molecules have been chemically linked to the surface of MWNTs.

### XRD Analysis

XRD patterns are used in further study of the changes in structure. Figure 3 shows XRD patterns obtained from pristine MWNTs and amino-functionalized MWNTs. There is a strong peak at $2\theta = 25.9°$ and two weak peaks at $2\theta = 42.6°$ and 53.4°

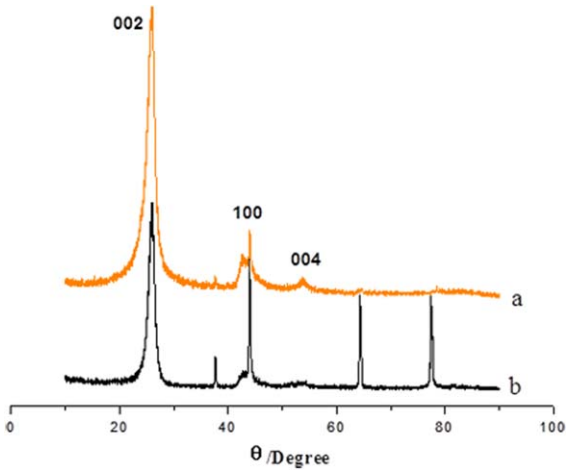


**Figure 3.** XRD analysis of MWNTs (a) m-MWNTs, (b) r-MWNTs. [Color figure can be viewed in the online issue, which is available at wileyonlinelibrary.com.]

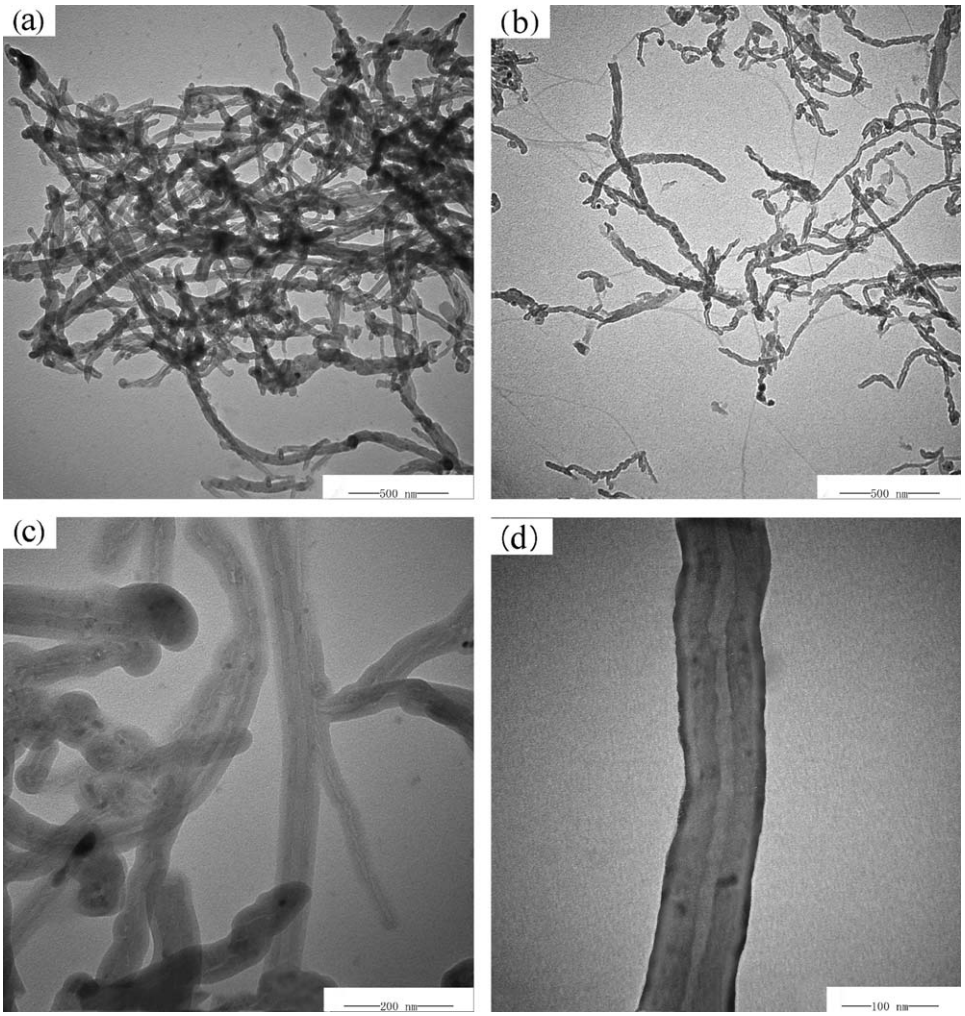


**Figure 4.** TEM images of MWNTs (a), r-MWNTs (b), a-MWNTs (c), m-MWNTs (low magnification), (d) m-MWNTs (high magnification).

in r-MWNTs, which in coordinate with the diffraction peaks of hexagonal of graphite at (002), (100), and the (004) crystal plane, indicating that the MWNT and graphite that have a similar structure.[31] The peaks at $2\theta = 64.3°$ and 77.9° correspond to elemental NiO and Ni, indicating that there exists some metal catalyst and metal oxide in r-MWNT. After amino-functionalization, the impurity peaks are disappeared. It is suggested that the impurities are completely removed. What's more, the peak becomes less sharper compared to the r-MWNT, indicating that the structure of amino-functionalization does not be destroyed, that is, it still has the same cylinder wall structure as r-MWNTs and interplanner spacing of all samples remains the same. It can be concluded that the modification process would not change the general structure of MWNTs. But a certain degree of orderliness reduces, which may be due to the introduction of a number of functional groups. The orderness decreased with the increasing defects on the sidewall and ports of the MWNTs.

### TEM Analysis

The microstructure of MWNTs dispersed in acetone is investigated by TEM, as shown in Figure 4. The surface of pristine MWNTs is relatively smooth and clean. After chemical modification, an extra phase appears on the sidewall of MWNTs. Figure 4(a) is the TEM image of r-MWNTs, it can be seen that r-MWNTs is long and has a smooth surface. They stack clutterly together and agglomerate seriously. There are many black spots in the structure of as-received MWNTs, which indicates that raw MWNTs contain some impurities, which can be explained by the reason that some metal catalysts is introduced in the preparation process of the MWNTs. Figure 4(b) shows that the surface of a-MWNTs is obviously rougher, and the length of carbon nanotubes is shorter. After $H_2SO_4/HNO_3$ treatment, there are few black spots in the structure of a-MWNTs, which means that most of the impurities have been removed. The agglomeration is inhibited in a certain degree, indicating carboxylated MWNTs is successful. Figure 4(c,d) are the m-MWNTs with low magnification and high magnification, respectively. The structure of m-MWNTs is a little indistinct. This may be due to the MPDA molecule grafting onto the MWNTs. Compared with r-MWNTs, m-MWNTs has a rougher surface and a larger diameter with a clear core-shell structure.[17] It is suggested that the surface of MWNTs is coated with a polymer chains, which is consistent with the results of FT-IR

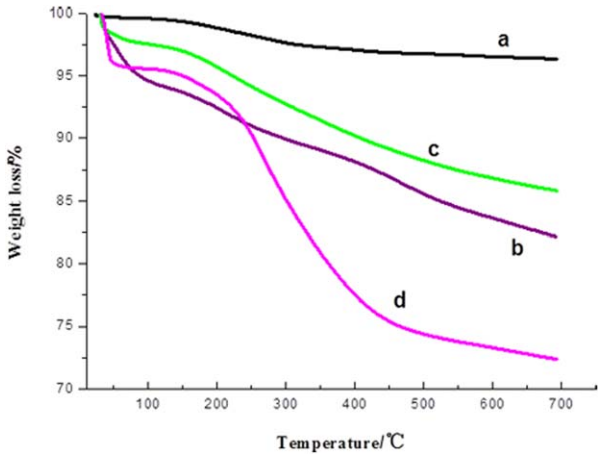


**Figure 5.** TGA curves of MWNTs in $N_2$, 10/min. (a) r-MWNTs, (b) a-MWNTs, (c) c-MWNTs, (d) m-MWNTs. [Color figure can be viewed in the online issue, which is available at wileyonlinelibrary.com.]

spectra. TEM analysis provides the direct evidence that the MPDA molecule is successfully grafted on the surface of MWNTs through the carboxylation, chloridation and amination by a covalent bond method, realizing the amino functionalized of MWNT.

### Thermogravimetric Analysis

Thermogravimetric (TGA) is one of the primary means to characterize the thermal stability and is performed in order to analyze the content of functionalized MWNTs. The TGA analysis conducted on as-received MWNTs and modified MWNTs are presented in Figure 5. As expected, the thermal degradation of MWNTs is a multistage process. TGA trace of raw MWNTs shows little weight loss, which is approximately 5% below 300°C. This may be attributed to some amorphous carbon and impurities in the r-MWNT.

The initial decomposition temperature of MWNTs decreases after treated by mixed acid. This is mainly due to —COOH, —OH functional groups caused by the oxidation of the MWNTs surface. The decomposition temperature of the functional groups is slower, and these functional groups damage the regularity of MWNTs surface, resulting in the lower decomposition temperature. The chloride treated MWNTs contains a lot of —COCl groups, so it is easy to decompose in the initial heating process. When the temperature is above 100°C, the curve has the similar trend as carboxyl-MWNT. Whereas, the onset temperature of amino functionalized MWNTs becomes dramatically lower, which is due to the fact that the additional organic functional groups are decomposed before the onset weight loss of MWNTs. There are two weight loss steps in the MPDA modified MWNTs below 500°C. In the first phase, thermal degradation in the range between 100 and 250°C may be explained by the elimination of carboxyl group and the unreacted chloride groups attached to the MWNTs walls. The weight loss of second stage is more obvious, which is caused by the decomposition of MPDA grafted on the surface of the MWNTs.[32] In addition, the grafting rate of amino groups can be obtained by comparing the decomposition of r-MWNTs. The mass fraction of the organic molecules grafted onto MWNTs is about 20 wt %.

TGA results show that MPDA is successfully grafted onto the MWNTs surface following by acidification, chloride and ammonia treatment, which is consistent with the results of FT-IR and TEM.

### Mechanical Properties

Figure 6 depicts the mechanical properties of the MWNTs/epoxy composites containing different MWNTs. Figure 6(a,b) are impact strength and flexural strength of the composite, respectively. With the increasing content of MWNTs, impact strength and flexural strength of the composites increase initially and then decrease. Among the three different kinds of composite materials, the amino MWNTs/epoxy composite shows the highest mechanical properties.

When the MWNTs content is 1.5 wt %, the impact strength and bending strength of the composite reach the maximum. Compared with the pure epoxy, impact strength of amino MWNTs/epoxy composite increases from 16.26 KJ/$m^2$ to 25.85 KJ/$m^2$ and bending strength increases from 104.3 MPa to 128.1

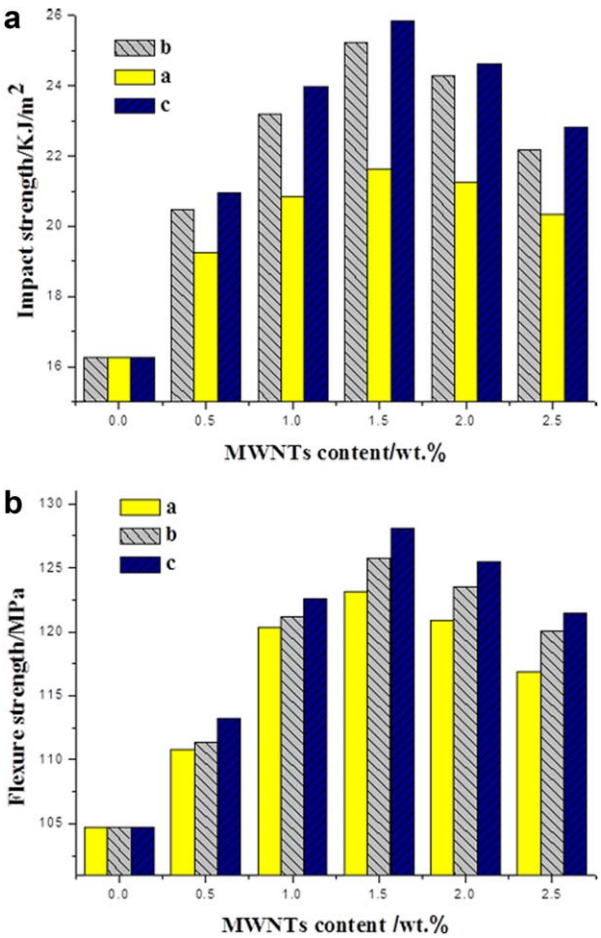


**Figure 6.** a. Effect of MWNTs content on impact strength of the MWNTs/epoxy composites (a) r-MWNTs/epoxy composites, (b) a-MWNTs/epoxy composites, (c) m-MWNTs/epoxy composites. b. Effect of MWNTs content on flexural strength of the MWNTs/epoxy composites (a) r-MWNTs/epoxy composites, (b) a-MWNTs/epoxy composites, (c) m-MWNTs/epoxy composites. [Color figure can be viewed in the online issue, which is available at wileyonlinelibrary.com.]

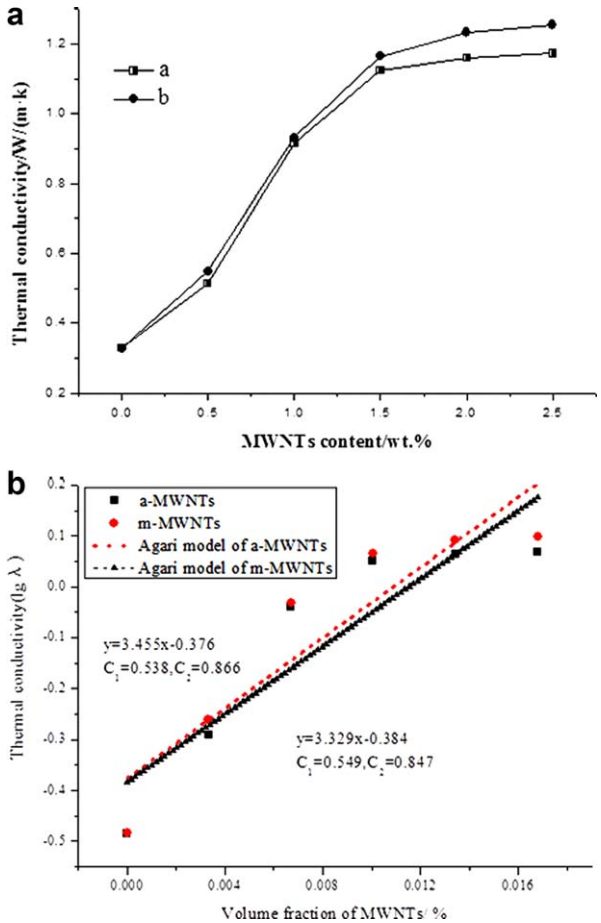


**Figure 7.** a. Thermal conductivity of MWNTs/epoxy composites (a) a-MWNTs/epoxy composites (b) m-MWNTs/epoxy composites. b. Thermal conductivity of MWNTs/epoxy composites as a function of volume fraction and the Agari model linear fitting results. [Color figure can be viewed in the online issue, which is available at wileyonlinelibrary.com.]

MPa, increased by 59% and 23%, respectively. However, when the content of MWNTs is 2 wt %, impact strength and flexural strength of the all the three composite materials reduce. Since the original surface energy of MWNTs can be very high and it is easy to agglomerate. When the addition amount is small, although agglomeration exists, the contribution of its high mechanical properties is much greater than agglomeration. When the dosage is increased, agglomeration becomes even more worse and the reunite dominants, so mechanical properties of the composite decrease.[33]

Whereas, when the functionalized MWNTs content is low, it can be better dispersed in the epoxy matrix and can effectively perform its excellent properties, so improves the strength of the composite material gradually. But when the filler content further increases, MWNTs slips each other which is caused by poor dispersion and leads to defects, resulting in function failure of interface between MWNTs and matrix. Finally affects the load transfer. Amino-MWNTs can increase the interface adhesion between MWNTs and matrix. What's more, it can be uniformly dispersed in the resin matrix. Therefore, amino MWNTs/epoxy composite material present better reinforcing effect.

### Thermal Conductivity

The experimentally determined thermal conductivity of MWNTs/epoxy composites, displayed as a function of filler content is shown in Figure 7. As can be seen from the Figure 7(a), thermal conductivity of the composite increases obviously with the increasing load of filler and the amino-functionalized MWNTs lead to the strongest improvement of thermal conductivity compared with the carboxylated one. When filling content of MWNTs is 2 wt %, the thermal conductivity of carboxylated and amino MWNTs/epoxy composite are 1.161 W/mK and 1.236 W/mK, respectively, which are approximately six times higher compared to the pure epoxy resin and meet the expected value.

In order to better understand the differences in the observed behavior, the conduction mechanism of the thermal transport should be considered. The observed phenomenon can be explained in terms of interfacial adhesion between the filler and the epoxy matrix. This reduces the air void volume, which is important because there is a very low thermal conductivity of air ($\lambda_{air} = 0.0024$ W/m K) at the filler-matrix interface. As the thermal conductivity of the composite filled with particles is not only related to the thermal conductivity of the fillers but also the interface thermal resistance. The MWNTs exhibit significantly higher thermal conductivity than the amorphous epoxy matrix due to the higher number of phonon vibrational modes and higher free length of path in the crystalline graphite structures. Furthermore, since the amino-MWNTs/epoxy has strong bonding force and the interface thermal resistance is small, so its thermal conductivity increases more obvious.

As also indicated in Figure 7(a), at a filler content of less than 0.5 wt % (equals to 0.003 vol %), the thermal conductivity of epoxy resin system increases slowly. the thermal conductivity of epoxy resin system increases rapidly, when added more than 0.5 wt % MWNTs. When filling amount is above 1.5 wt %, the increasing rate of thermal conductivity remains stable. This can be explained by the established percolation theory,[34,35] with an onset conductivity when a critical filler concentration, commonly named percolation threshold, is reached to form conductive ways. Initially, MWNTs is segregated or encapsulated completely by epoxy matrix with lower filling amount, and cannot form an effective heat transfer path. With further increment of the filler, MWNTs in the resin matrix start to contact with each other and form heat conduction path.[12] And then the heat can be delivered effectively, so thermal conductivity of the system increases. However, when the filling content is too high, most of MWNTs has been connected to each other and the amount of heat conduction path is tend to be saturated, it is not obvious to further improve thermal conductivity with more filler, so the thermal conductivity of composite materials began to increase slowly.

In order to predict the thermal conductivity of composites as a function of the volume fraction of the filler, the Agari model[36] is used here to evaluate the thermal conductivity of composites among many theoretical models published. Agari model considers the effect of dispersion state by introducing two factors $C_1$ and $C_2$:

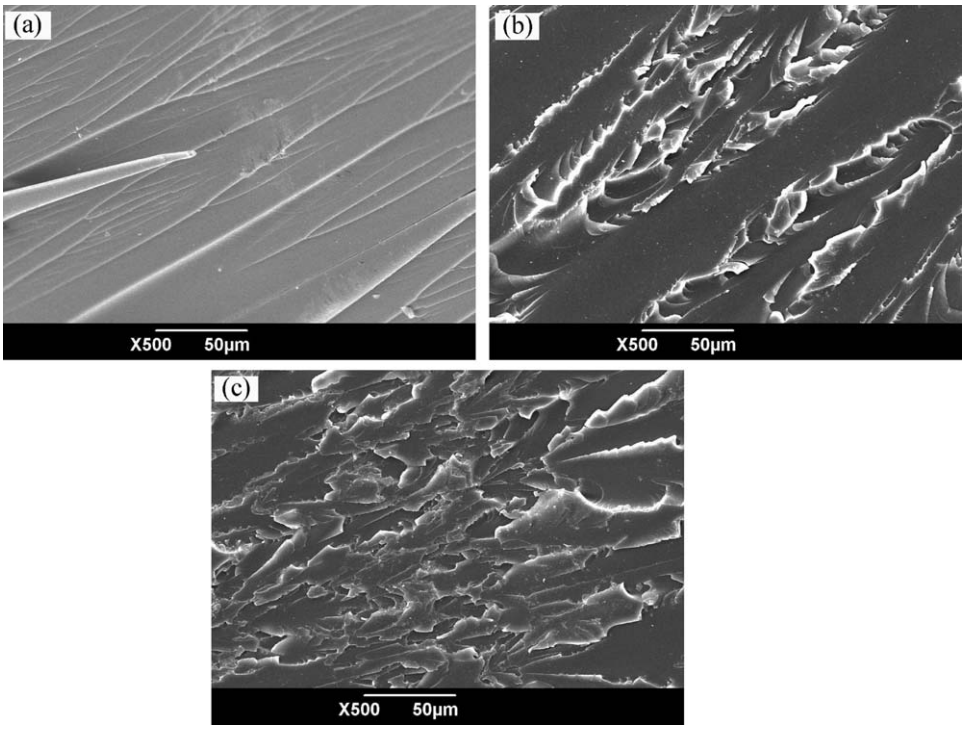


**Figure 8.** SEM image of the fracture surface of pure epoxy and MWNTs/epoxy composites cured by EMI-2,4 (a) pure epoxy, (b) a-MWNTs/epoxy composites, (c) m-MWNTs/epoxy composites.

$$\mathrm{Lg}\lambda = V_f C_2 \mathrm{lg}\lambda_f + (1-V_f)\ \mathrm{lg}(C_1\lambda_p)$$

where $\lambda$, $\lambda_p$, and $\lambda_f$ are the thermal conductivity of composites, polymer and filler, respectively; $V_f$ is the volume fraction of filler; $C_1$ is a factor relating to the structure of polymer, such as crystallinity of the matrix, and $C_2$ is a factor relating to the measure of ease for the formation of conductive chains of filler. According to Agari, the range of $C_2$ should between 0 and 1, the closer $C_2$ value is to 1, the more easily conductive chains are formed in composites.[1] As can be seen from Figure 7(b), the divergence from experimentally obtained results, which find lower thermal conductivity, can be explained by the restriction of their model to volumetric effects. By fitting the experimental data into the model, $C_1$ and $C_2$ for the two systems are present in the Figure 7(b). It can be observed that $C_2$ value of the amino-functionalization of MWNTs is larger than the carboxylated one, which means the more easily conductive chains are formed in composites.

As is known to all, the transport of heat in all non-metals is by the flow of lattice vibration energy.[37] For a two phase system like MWNTs/epoxy composites, interfacial physical contact between polymer and filler is very critical, since phonons are very sensitive to surface defects.[38] Thermal resistance is caused by various types of phonon scattering processes, and the interfacial thermal barriers in composites is mainly due to the scattering of phonons resulting from acoustic mismatch and flaw associated with the matrix-filler interface.[39] The interface between the two-phase composites acts as a barrier of heat transmission. So the surface treatment of MWNTs with amino groups improves the interfacial bonding between MWNTs and matrix, and reduces the voids at the filler-matrix interface, which facilitates enhancing the thermal conductivity. The significantly enhancement of thermal conductivity with the increasing filler content was observed with our experimental data compared with those which filled with 1 wt % m-MWNTs only increased to 0.344 W/mK obtained by Kwon et al.[9]

The phenomenon indicates that MPDA functionalization improves the interfacial heat transport and phonon conduction by reducing the boundary scattering losses between the epoxy matrix and the MWNTs, and facilitates better dispersion of MWNTs in the matrix, which is beneficial to the enhancement of the thermal conductivity of MWNTs/epoxy composites.[40]

### SEM Analysis

In order to analyze the cross section of the composite, the SEM micrographs are carried out. SEM micrographs of pure epoxy resin and MWNTs/epoxy composites filled with 1wt % MWNTs are shown in Figure 8. As can be seen in Figure 8(a), the cross section of pure epoxy is smooth and the crack is uniform and orderly. It tends to be a dendritic dispersion, indicating that the process of the expansion crack resistance is small and the energy loss is small. That is to say, the impact strength is low, which belongs to a typical brittle fracture. Figure 8(b) is the impact fracture of the carboxylated-MWNTs/epoxy composite filled with 1 wt % MWNTs. We can see the cross section tend to be rough and uneven, and the crack is scaly. The reason is that carboxylated-MWNTs can induce crazing. When subjected to shock loading, crack can spread energy through crazing and

increase the energy absorbed by the resin, thereby enhancing the toughness.[41] The cracks in Figure 8(c) are smaller and irregular. What is more, it can be seen that amino-MWNTs is uniformly dispersed in the resin system. This is because the introduction of the amino group not only improves the dispersion of MWNTs in the matrix and also involves in the curing reaction of epoxy resin. With a covalent bond between the two connections, the binding force between MWNTs and the matrix is effectively improved, therefore, effectively prevents the growth of micro cracks.

The analysis above shows that, MWNTs can prevent rapid expansion of macroscopic crack in matrix. In the meanwhile, cracks become disordered and consume part of the energy. The macroscopic mechanical properties of the composite with carboxylated and amino-MWNTs are well improved compared with the pure epoxy.

## SUMMARY AND CONCLUSIONS

In order to obtain uniform dispersion of MWNTs in the epoxy matrix, improving the thermal conductivity and mechanical properties of MWNTs/epoxy composites, MWNTs functionalized by MPDA molecule are carried out. After functionalization, better dispersion of the MWNTs in the matrix is obtained and the thermal conductivity of the composite is six times higher than the pure epoxy matrix only with 2 wt % MWNTs. These functionalized MWNTs actually improve the affinity to the epoxy resin matrix and a heat flow network has been developed by strong chemical covalent bonds between MWNTs and epoxy resins.

During the functionalization process, mixed acid ($H_2SO_4$/$HNO_3$) treatment of MWNTs should be first executed to effectively generate carboxyl groups on their surface. FT-IR analysis results confirm that the introduction of carboxyl groups by $H_2SO_4$/$HNO_3$ treatment is successful and MPDA molecule used in this study is chemically grafted on the surface of MWNTs. XRD analysis indicates that chemical functionalization decreases the crystalline content of MWNTs and the impurities are completely removed. However, it does not greatly disrupt their structure. HRTEM analysis indicates that MPDA is grafted onto the MWNTs surface to form a thin polymer-layer. Rougher surface and larger diameter with a clear core-shell structure are obtained after modification, which is beneficial for better dispersion in epoxy matrix. Thermo gravimetric analysis suggests that the initial decomposition temperature of MWNTs decreases after treated by mixed acid. The onset temperature of amino functionalized MWNTs becomes dramatically lower and the mass fraction of the functional molecules grafted onto MWNTs is about 20 wt %.

The thermal conductivity increased with an increase in filling amount. The thermal conductivity of carboxylated and amino MWNTs/epoxy composite filled with 2 wt % MWNTs are 1.161 W/mK and 1.236 W/mK, respectively. The thermal conductivity of the amino functionalized one meets the requirement of the microelectronics applications. The high thermal conductivity obtained at low filler loading can be ascribed to the fact that a networked dispersion state of MWNTs existed in the composites, which acted as conductive channels. The mechanical properties of MWNTs/epoxy composites are improved after functionalization, which is due to better dispersion in the matrix and the enhancement of interface adhesion between MWNTs and matrix. Compared with the pure epoxy, impact strength of amino MWNTs/epoxy composite increases from 16.26 KJ/m$^2$ to 25.85 KJ/m$^2$ and bending strength increases from 104.3 MPa to 128.1 MPa, increased by 59% and 23%, respectively. The morphology characterization of MWNTs/epoxy composite shows that the fracture patterns is changed from brittle fracture to ductile fracture and the amino functionalized MWNTs are homogeneously dispersed in epoxy matrix.

## ACKNOWLEDGMENTS

The authors are sincerely grateful for the help of Ms. Zhang for the SEM photograph. The authors also appreciate the companies and relatives who friendly offered the materials and helpful.

## REFERENCES

1. Zhou, W.; Wang, C.; Ai, T.; Wu, K.; Zhao, F.; Gu, H. *Compos. A* **2009**, *40*, 830.
2. Ekpu, M.; Bhatti, R.; Okereke, M. I.; Mallik, S.; Otiaba, K. *Microelectron. J.* **2014**, *45*, 159.
3. Iijima, S. *Nature* **1991**, *354*, 56.
4. Dos Santos, M. N.; Opelt, C. V.; Lafratta, F. H.; Lepienski, C. M.; Pezzin, S. H.; Coelho, L. A. F. *Mater. Sci. Eng. A* **2011**, *528*, 4318.
5. Chen, X.; Wang, J.; Lin, M.; Zhong, W.; Feng, T.; Chen, X.; Chen, J.; Xue, F. *Mater. Sci. Eng. A* **2008**, *492*, 236.
6. Tonpheng, B.; Yu, J.; Andersson, O. *Macromolecules* **2009**, *42*, 9295.
7. Im, H.; Kim, J. *Carbon* **2012**, *50*, 5429.
8. Abrar, M.; Farwa, G. U.; Naseer, S.; Saeed, A.; Khan, A. W.; Iqbal, Z.; Hussain, S. T.; Zakaullah, M. *Curr. Appl. Phys.* **2013**, *13*, 567.
9. Kwon, Y.; Yim, B.-S.; Kim, J.-M.; Kim, J. *Microelectron Reliab.* **2011**, *51*, 812.
10. Abdalla, M.; Dean, D.; Robinson, P.; Nyairo, E. *Polymer* **2008**, *49*, 3310.
11. Hong, J.; Park, D. W.; Shim, S. E. *Macromol. Res.* **2012**, *20*, 465.
12. Zhou, W. *Thermochim. Acta* **2011**, *512*, 183.
13. Zhu, J.; Peng, H.; Rodriguez-Macias, F.; Margrave, J. L.; Khabashesku, V. N.; Imam, A. M.; Lozano, K.; Barrera, E. V. *Adv. Funct. Mater.* **2004**, *14*, 643.
14. Shen, J.; Huang, W.; Wu, L.; Hu, Y.; Ye, M. *Compos. Sci. Technol.* **2007**, *67*, 3041.
15. Yang, S. Y.; Ma, C. C. M.; Teng, C. C.; Huang, Y. W.; Liao, S. H.; Huang, Y. L.; Tien, H. W.; Lee, T. M.; Chiou, K. C. *Carbon* **2010**, *48*, 592.
16. Qu, Z. H.; Wang, G. J. *J. Nanosci. Nanotechnol.* **2012**, *12*, 105.
17. Chang, C.-M.; Liu, Y.-L. *Carbon* **2009**, *47*, 3041.

18. Najafi, E.; Kim, J. Y.; Han, S. H.; Shin, K. *Colloid Surf. A* **2006**, *284*, 373.
19. Hussain, S.; Amade, R.; Jover, E.; Bertran, E. *J. Mater. Sci.* **2013**, *48*, 7620.
20. Lee, J. H.; Hong, B.; Park, Y. S. *Thin Solid Films* **2013**, *546*, 77.
21. Valentini, L.; Puglia, D.; Carniato, F.; Boccaleri, E.; Marchese, L.; Kenny, J. M. *Compos. Sci. Technol.* **2008**, *68*, 1008.
22. Yang, K.; Gu, M.; Jin, Y.; Mu, G.; Pan, X. *Compos. A* **2008**, *39*, 1670.
23. Yang, K.; Gu, M.; Guo, Y.; Pan, X.; Mu, G. *Carbon* **2009**, *47*, 1723.
24. Shen, J.; Huang, W.; Wu, L.;Hu, Y.; Ye, M. *Mater. Sci. Eng. A: A* **2007**, *464*, 151.
25. Datsyuk, V.; Lisunova, M.; Kasimir, M.; Trotsenko, S.; Gharagozloo-Hubmann, K.; Firkowska, I.; Reich, S. *Applied Physics A* **2011**, *105*, 781.
26. Teng, C.-C.; Ma, C.-C. M.; Yang, S.-Y.; Chiou, K.-C.; Lee, T.-M.; Chiang, C.-L. *J. Appl. Polym. Sci.* **2012**, *123*, 888.
27. Zhao, C.; Ji, L.; Liu, H.; Hu, G.; Zhang, S.; Yang, M.; Yang, Z. *J. Solid State Chem.* **2004**, *177*, 4394.
28. Wang, Y.; Iqbal, Z.; Malhotra, S. V. *Chem. Phys. Lett.* **2005**, *402*, 96.
29. Zhu, J.; Kim, J.; Peng, H.;Margrave, J. L.; Khabashesku, V. N.; Barrera, E. V. *Nano Lett.* **2003**, *3*, 1107.
30. Yan, D.; Yang, G. *Mater. Lett.* **2009**, *63*, 298.
31. Stamatin, I.; Morozan, A.; Dumitru, A.; Ciupina, V.; Prodan, G.; Niewolski, J.; Figiel, H. *Phys. E* **2007**, *37*, 44.
32. Yang, S.-Y.; Ma, C.-C. M.; Teng, C.-C.; Huang, Y.-W.; Liao, S.-H.; Huang, Y.-L.; Tien, H.-W.; Lee, T.-M.; Chiou, K.-C. *Carbon* **2010**, *48*, 592.
33. Shen, J.; Huang, W.; Wu, L.; Hu, Y.; Ye, M. *Compos. A* **2007**, *38*, 1331.
34. Kirkpatrick, S. *Rev. Modern Phys.* **1973**, *45*, 574.
35. Gojny, F. H.; Wichmann, M. H. G.; Fiedler, B.; Kinloch, I. A.; Bauhofer, W.; Windle, A. H.; Schulte, K. *Polymer* **2006**, *47*, 2036.
36. Agari, Y.; Ueda, A.; Nagai, S. *J. Appl. Polym. Sci.* **1993**, *49*, 1625.
37. He, Y.; Moreira, B. E.; Overson, A.; Nakamura, S. H.; Bider, C.; Briscoe, J. F. *Thermochim. Acta* **2000**, *357*, 1.
38. Davis, L. C.; Artz, B. E. *J. Appl. Phys.* **1995**, *77*, 4954.
39. Youngblood, G.; Senor, D. J.; Jones, R.; Graham, S. *Compos. Sci. Technol.* **2002**, *62*, 1127.
40. Yang, K.; Gu, M. *Compos. A* **2010**, *41*, 215.
41. Xu, J.; Yao, P.; Jiang, Z.; Liu, H.; Li, X.; Liu, L.; Li, M.; Zheng, Y. J. *Appl. Polym. Sci.* **2012**, *125*, E334.